

# Permutation Invariant Likelihoods and Equivariant Transformations

Chris Bender<sup>\*1</sup> Juan Jose Garcia<sup>\*2</sup> Kevin O'Connor<sup>\*3</sup> Junier B. Oliva<sup>1</sup>

## Abstract

In this work, we fill a substantial void in machine learning and statistical methodology by developing extensive generative density estimation techniques for exchangeable non-*i.i.d.* data. We do so through the use of permutation invariant likelihoods and permutation equivariant transformations of variables. These methods exploit the intradependencies within sets in ways that are independent of ordering (for likelihoods) or order preserving (for transformations). The proposed techniques are able to directly model exchangeable data (such as sets) without the need to account for permutations or assume independence of elements. We consider applications to point clouds and provide several interesting experiments on both synthetic and real-world datasets.

## 1. Introduction

Modeling non-*i.i.d.*, exchangeable (unordered) data is a fundamental problem. Sets with complicated intrinsic relationships are ubiquitous in our world, thus it is critical to consider dependencies among points when modeling collections of data.

For instance, each member of a social-circle behaves in ways which depend strongly on both their previous actions as well as actions of the other members. Similarly, the forces of galaxies within a cluster yield a rich web of relations depending on the characteristics of each constituent piece of matter. Yet, the bulk of machine learning approaches either ignore the relation between points (*i.i.d.* methods) (Qi et al., 2017) or model dependencies in a manner that depends on orderings (sequential methods) (Rezatofghi et al., 2017; You et al., 2018).

In this work we develop generative methods that are in-

<sup>\*</sup>Equal contribution <sup>1</sup>Department of Computer Science, University of North Carolina, Chapel Hill, NC 27510 <sup>2</sup>Facultad de Ingeniería en Electricidad y Computación, Escuela Superior Politécnica del Litoral, ESPOL, Ecuador <sup>3</sup>Department of Statistics and Operations Research, University of North Carolina, Chapel Hill, NC 27510. Correspondence to: Chris Bender <bender@cs.unc.edu>.

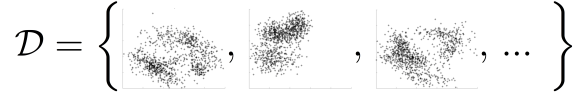


Figure 1. Training dataset of sets. Here each instance  $\mathbf{X}_i$  is a set of points  $\mathbf{X}_i = \{x_{i,j} \in \mathbb{R}^d\}_{j=1}^{n_i}$ . We look to estimate  $p(\mathbf{X}_i)$ ; that is we make a generative model that generates distinct sets.

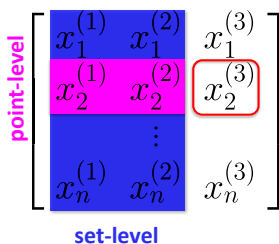
herently unordered and malleable to inputs of varying size, whilst modeling dependencies among points. We apply our methods to modeling entire sets at a time.<sup>1</sup> That is, rather than modeling a single data point  $x \in \mathbb{R}^d$  as  $p(x)$  given a training-set of points  $\mathcal{D} = \{x_i \in \mathbb{R}^d\}_{i=1}^N$ , here we look to model an entire set of points  $p(\{x_j\}_{j=1}^{n_i})$  given a training-set of sets  $\mathcal{D} = \{\mathbf{X}_i\}_{i=1}^N$ , where  $\mathbf{X}_i = \{x_{i,j} \in \mathbb{R}^d\}_{j=1}^{n_i}$  is a set of  $n_i$  points (see Figure 1). For instance, in the case of modeling point clouds,  $\mathbf{X}_i$  may be a set of  $3d$  points sampled from an object’s surface.

In most implementations, a set  $\mathbf{X} = \{x_j\}_{j=1}^{n_i}$  will be observed in some particular order  $(x_1, \dots, x_n)$ . For instance, when  $\mathbf{X}$  is stored as a  $n \times d$  matrix,  $\mathbf{x} \in \mathbb{R}^{n \times d}$ ,  $(x_1, \dots, x_n)$  is determined by the rows of  $\mathbf{x}$ ; however, the ordering is arbitrary as the underlying instance  $\mathbf{x}$  is a set and has no intrinsic order. Often, techniques shoehorn invariances to observed orderings by feeding randomly permuted data into sequential models (Rezatofghi et al., 2017; You et al., 2018). Such techniques attempt to average out the likelihood of the model over all permutations:

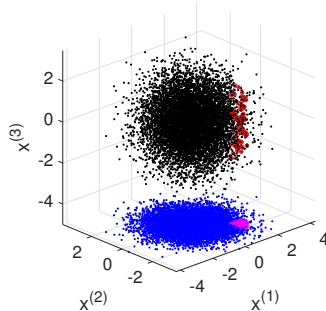
$$p(\{x_1, \dots, x_n\}) = \frac{1}{n!} \sum_{\pi} p_s(x_{\pi_1}, \dots, x_{\pi_n}), \quad (1)$$

where  $p_s$  is some sequential model. Of course, the combinatorial nature of permutations renders the observation of all potential combinations for even a small collection of points infeasible. Furthermore, there are often no guarantees that the learned sequential model,  $p_s$ , fed data in this manner, will learn to ignore orderings. This may be especially so for unseen test data (Vinyals et al., 2015).

<sup>1</sup>We use the following notational conventions: bold capitals, e.g.  $\mathbf{X}$ , corresponds to a set of multiple points; bold lowercase, e.g.  $\mathbf{x}$ , corresponds to a matrix representation of a set; math italics, e.g.  $x$ , corresponds to a multivariate point; and  $x_i^{(j)}$  corresponds to the  $j$ th dimension of the  $i$ th point of a set.



(a) Matrix view of a 3d set



(b) Scatter plot of a 3d input set

Figure 2. (a) Matrix and (b) scatter plot views of a set. Although one may permute rows (points) of the matrix, the underlying set is unchanged (as it is unordered). Thus, we must make sure that our model is invariant to permutations. However, we would like to capture both aggregate set-level (blue) and point-level (magenta) dependencies present in the set, for instance when modeling  $x_2^{(3)}$  (red).

In this work, we build non-*i.i.d.*, exchangeable models from the ground up for a principled and novel approach to capture intradependencies of points in an unordered fashion. We shall develop density estimates that are permutation invariant:

$$\forall \pi, p(x_1, \dots, x_n) = p(x_{\pi_1}, \dots, x_{\pi_n}). \quad (2)$$

This property is invaluable for unordered collections such as sets as they represent an equivalence class over permutations. Rather than averaging the likelihood over the equivalence class as (1), a permutation invariant likelihood (2) yields the same value over the equivalence class. A simple method to achieve exchangeability is to impose an *i.i.d.* assumption:

$$p(x_{\pi_1}, \dots, x_{\pi_n}) = \prod_{i=1}^n p(x_i). \quad (3)$$

However, the *i.i.d.* assumption imposes that the model not account any dependencies among points. Furthermore, an *i.i.d.* approach is often unable to model multiple distinct collections since points will be drawn independently from an identical distribution. Modeling a set in an *i.i.d.* fashion fails even in the simple case where sets are drawn from one of distinct two distributions, e.g.:

$$\begin{aligned} p(x_1, \dots, x_n) \\ = \frac{1}{2}p_1(x_1, \dots, x_n) + \frac{1}{2}p_2(x_1, \dots, x_n). \end{aligned} \quad (4)$$

The key challenge, and our main contribution, is the development of techniques that are able to naturally model dependencies between points in an unordered manner.

Throughout this work, we make use of the notion of *point-level* and *set-level* information, both of which are crucial to generating exchangeable data. Figure 2 illustrates the use of set- and point-level information in both graphical and matrix form. Point-level information refers to the correlations

among dimensions of points, e.g.  $p(x^{(j)} \mid x^{(<j)})$ . This common notion is often the sole focus of generative methods as they ignore any intradependence among points, and only attempt to capture the dependencies across dimensions. In addition to point-level information, we also consider set-level information, which is the aggregate descriptor of points in a collection. As we capture the dependencies among points of the same set in an unordered fashion, we must consider aggregate descriptors of points within a modeled set; e.g. a set statistic,  $T(\mathbf{x})$ .

Below, we expound upon our methodology for creating likelihoods that are unordered while still modeling intradependencies among points. Particularly, we develop a framework we coin PILET: Permutation Invariant (conditional) Likelihoods and Equivariant Transformations of variables. We propose several novel transformations of sets and methods for conditioning likelihoods and illustrate these methods in synthetic and real-world point cloud data.

## 2. Methods

Following (Oliva et al., 2018), we jointly develop two components that are common to many modern density estimation techniques: a transformation of variables (Dinh et al., 2014; 2016; Kingma & Dhariwal, 2018), and an autoregressive likelihood (Larochelle & Murray, 2011; Uria et al., 2013; 2016; Gregor et al., 2014; Germain et al., 2015). In order to preserve exchangeability, we expand on permutation equivariant transformations (Zaheer et al., 2017) and permutation invariant conditional likelihoods in the resulting latent space. That is, for a permutation operator,  $\Gamma$ , on a sequence of  $n$   $d$ -dimensional point,  $\mathbf{x} \in \mathbb{R}^{n \times d}$ , we develop: one, transformations,  $q : \mathbb{R}^{n \times d} \mapsto \mathbb{R}^{n \times d}$ , such that

$$q(\Gamma \mathbf{x}) = \Gamma q(\mathbf{x}), \quad (5)$$

which yields a permutation equivariant mapping; two, likelihoods,  $p(\mathbf{x}) : \mathbb{R}^{n \times d} \mapsto \mathbb{R}_{\geq 0}$  such that,

$$p(\Gamma \mathbf{x}) = p(\mathbf{x}), \quad (6)$$

which yields a permutation invariant mapping. We will see that (5) and (6) guarantee an exchangeable model.

## 2.1. Background

We briefly discuss Deepset architectures (Zaheer et al., 2017) and Transformation Autoregressive Networks (Oliva et al., 2018) which are used in the construction of our models.

### 2.1.1. DEEPSETS

We make extensive use of permutation invariant representations of sets. We construct a set embedding  $\varphi(\mathbf{x}) \in \mathbb{R}^s$  such that  $\varphi(\Gamma \mathbf{x}) = \varphi(\mathbf{x})$  for all permutation operations  $\Gamma$ . Hence,  $\varphi(\mathbf{x})$  shall express a true representation of the underlying (unordered) set. To construct these set embeddings  $\varphi(\mathbf{x})$ , we use Deepset layers (Zaheer et al., 2017). Deepset layers are composed of multiple permutation equivariant mappings such as:

$$\{y_i\}_{i=1}^n \mapsto \{\phi(y_i) - \max_j \phi(y_j)\}_{i=1}^n, \quad (7)$$

for  $y \in \mathbb{R}^m$  (some intermediate embedding of  $\mathbf{x}$ ), mapping (of a fully connected network)  $\phi : \mathbb{R}^m \mapsto \mathbb{R}^s$ , and element-wise max. The final output set embedding is the global pool of the last permutation equivariant output  $\{y'_i\}_{i=1}^n$ , e.g.  $\frac{1}{n} \sum_{i=1}^n y'_i \in \mathbb{R}^s$ .

### 2.1.2. TRANSFORMATION AUTOREGRESSIVE NETWORKS (TAN)

We also make use of transformations of variables and autoregressive conditionals jointly as described in the TAN framework (Oliva et al., 2018). For a  $d$  dimensional distribution over real-valued covariates  $x = (x^{(1)}, \dots, x^{(d)})$  we may write a density in terms of an invertible transformation of variables  $z = q(x)$  and the chain rule on  $z$  as follows:

$$p(x^{(1)}, \dots, x^{(d)}) = \left| \det \frac{dq}{dx} \right| \prod_{i=1}^d p(z^{(i)} | z^{(<i)}) \quad (8)$$

where  $|\det \frac{dq}{dx}|$  is the Jacobian of the transformation  $q$ . We extend from single  $d$  dimensional points to sets of  $n$   $d$  dimensional points as:

$$p(\mathbf{x}_1, \dots, \mathbf{x}_n) = \left| \det \frac{dq}{d\mathbf{x}} \right| \prod_{i=1}^n p(\mathbf{z}^{(i)} | \mathbf{z}^{(<i)}), \quad (9)$$

where  $\mathbf{z} = q(\mathbf{x})$ ,  $\mathbf{z}^{(i)} \in \mathbb{R}^{n \times 1}$  is the (column) vector of the  $i$ th covariate of all  $n$  points,  $\mathbf{z}^{(<i)} \in \mathbb{R}^{n \times i-1}$  is the matrix of

the first  $i-1$  covariates of points,  $q : \mathbb{R}^{n \times d} \mapsto \mathbb{R}^{n \times d}$  is permutation equivariant (5), and  $p(\mathbf{z}^{(i)} | \mathbf{z}^{(<i)})$  is permutation invariant (6), e.g.  $\forall \Gamma, p(\mathbf{z}^{(i)} | \mathbf{z}^{(<i)}) = p(\Gamma \mathbf{z}^{(i)} | \Gamma \mathbf{z}^{(<i)})$ . It is straightforward to show that (9) results in a permutation invariant likelihood.

**Theorem 2.1.** (9) preserves exchangeability.

*Proof.* Let  $\Gamma$  be a permutation and suppose that the data  $\mathbf{x}$  is exchangeable. As the transformation  $q$  is defined to be permutation equivariant, we have  $q(\Gamma \mathbf{x}) = \Gamma q(\mathbf{x})$ . Thus  $|\det \frac{dq}{d\mathbf{x}}|$  is invariant to  $\Gamma$ . Furthermore,

$$\begin{aligned} p(q(\Gamma \mathbf{x})^{(i)} | q(\Gamma \mathbf{x})^{(<i)}) &= p(\Gamma q(\mathbf{x})^{(i)} | \Gamma q(\mathbf{x})^{(<i)}) \quad (10) \\ &= p(q(\mathbf{x})^{(i)} | q(\mathbf{x})^{(<i)}), \quad (11) \end{aligned}$$

by the permutation equivariance of  $q$  and permutation invariance of  $p$ . Hence, the total set likelihood (9) is permutation invariant.  $\square$

Thus, the proposed model preserves the unordered structure of the input sets without the need for averaging over each permutation or assuming independence between elements.

## 2.2. Transformations

First, we develop several novel transformations  $q$  that are permutation equivariant (5). A simple permutation equivariant transformation is to transform each element of a set identically and independently:

$$(x_1, \dots, x_n) \mapsto (q(x_1), \dots, q(x_n)). \quad (12)$$

However, this transformation is unable to capture any dependencies between points, and operates in a *i.i.d.* fashion. Instead, we propose equivariant transformations that transform each element of a set in a way that depends on other points in the set, yielding a richer family of models. In other words, transforming as

$$(x_1, \dots, x_n) \mapsto (q(x_1, \mathbf{x}), \dots, q(x_n, \mathbf{x})). \quad (13)$$

Below, we propose several novel equivariant transformations with intra-set dependencies.

### 2.2.1. LINEAR PERMUTATION EQUIVARIANT (L-PEQ)

We start with a linear permutation equivariant transformation. It can be shown (Zaheer et al., 2017) that any linear permutation equivariant map of one dimensional points can be written in the form,  $\mathbf{x} \mapsto (\lambda \mathbf{I} + \gamma \mathbb{1} \mathbb{1}^T) \mathbf{x}$  for some scalars  $\lambda$  and  $\gamma$ , and  $\mathbf{x} \in \mathbb{R}^{n \times 1}$ . Specifically, a linear permutation equivariant transformation is the result of a matrix multiplication with identical diagonal elements and off diagonal elements.

Such a transformation captures intradependencies by mapping the  $j$ th dimension of the  $i$ th point as

$$x_i^{(j)} \mapsto \lambda^{(j)} x_i^{(j)} + \frac{\gamma^{(j)}}{n} \sum_{k=1}^n x_k^{(j)}, \quad (14)$$

incorporating the mean of other points in the set. We use the mean rather than the sum as in (Zaheer et al., 2017) because it allows for better symmetry with our proposed generalization in Sec. 2.2.2. It is trivial to go between the two formulations by scaling  $\gamma^{(j)}$  by  $n$ . The log-determinant of the transformation (14) can be shown to be  $(n-1) \log |\lambda^{(j)}| + \log |\lambda^{(j)} + \gamma^{(j)}|$ , and is invertible whenever  $\lambda^{(j)} \neq 0$  and  $\lambda^{(j)} + \gamma^{(j)} \neq 0$  with inverse:

$$z_i^{(j)} \mapsto \frac{z_i^{(j)}}{\lambda^{(j)}} - \frac{\gamma^{(j)}}{n\lambda^{(j)}(\lambda^{(j)} + \gamma^{(j)})} \sum_{k=1}^n z_k^{(j)}$$

### 2.2.2. NONLINEAR WEIGHTING (NW-PEQ)

We propose a generalization of the linear permutation equivariant transformation (14) here. Instead of a direct mean, we propose to weight each element by some nonlinear function that depends on the element's value relative to a global operation over the set:

$$\begin{aligned} x_i^{(j)} &\mapsto \lambda^{(j)} x_i^{(j)} + \gamma^{(j)} \frac{\sum_k x_k^{(j)} w(x_k^{(j)})}{\sum_m w(x_m^{(j)})} \\ &\mapsto \lambda^{(j)} x_i^{(j)} + \gamma^{(j)} \eta^{(j)} \end{aligned} \quad (15)$$

where  $w$  is the nonlinear weighting function and  $\eta^{(j)}$  is the weighted mean. The log-determinant of the Jacobian can be expressed as

$$\begin{aligned} \log |J| &= (n-1) \log |\lambda^{(j)}| \\ &+ \log \left| \lambda^{(j)} + \gamma^{(j)} \left( 1 + \frac{\sum_k (x_k^{(j)} - \eta^{(j)}) w'(x_k^{(j)})}{\sum_m w(x_m^{(j)})} \right) \right| \end{aligned} \quad (16)$$

where  $w'$  is the first derivative of  $w$ . It is clear that (16) simplifies to the linear determinant for constant  $w$ . Attempting to invert (15) results in an implicit function for  $\eta^{(j)}$

$$\eta^{(j)} = \left( 1 + \gamma^{(j)} \right)^{-1} \frac{\sum_k x_k^{(j)} w(x_k^{(j)} - \gamma^{(j)} \eta^{(j)})}{\sum_m w(x_m^{(j)} - \gamma^{(j)} \eta^{(j)})} \quad (17)$$

(where  $\lambda^{(j)}$  has been dropped for brevity) that could be solved numerically to perform the inverse for a general nonlinear weight. This formulation implies that the weighted permutation equivariant transform can be inverted even if  $w$  is not an invertible function. Thus, allowing for a larger family of nonlinearities than is typically included in transformative likelihood estimators (Dinh et al., 2014; 2016; Kingma & Dhariwal, 2018).

The simplest method forward is to choose a weighting function such that a sum of function inputs decomposes into a product of outputs, e.g.  $w(a+b) = f(a)f(b)$  where  $f$  is some nonlinear function. In this case, (17) simplifies to

$$\eta^{(j)} = \left( 1 + \gamma^{(j)} \right)^{-1} \frac{\sum_k x_k^{(j)} f(x_k^{(j)})}{\sum_m f(x_m^{(j)})} \quad (18)$$

and the inverse transform proceeds trivially. Choosing  $f$  to be the exponential function allows for the simplification, guarantees positive weights, and results in a softmax-weighted mean,

$$x_i^{(j)} \mapsto \lambda^{(j)} x_i^{(j)} + \gamma^{(j)} \frac{\sum_k x_k^{(j)} \exp(\beta^{(j)} x_k^{(j)})}{\sum_m \exp(\beta^{(j)} x_m^{(j)})} \quad (19)$$

with inverse temperature scaling  $\beta$ . It is apparent that this transformation reduces to the L-PEq transformation when  $\beta = 0$ . Additionally, in the limit as  $\beta \rightarrow \infty$  or  $\beta \rightarrow -\infty$ , the transformation tends to shift by the maximum or minimum of the set, respectively. The log-determinant of this transformation is identical to the linear case and the inverse comes directly from (18):

$$z_i^{(j)} \mapsto \frac{z_i^{(j)}}{\lambda^{(j)}} - \frac{\gamma^{(j)}}{\lambda^{(j)}(\lambda^{(j)} + \gamma^{(j)})} \frac{\sum_k z_k^{(j)} \exp(\frac{\beta^{(j)} z_k^{(j)}}{\lambda^{(j)}})}{\sum_m \exp(\frac{\beta^{(j)} z_m^{(j)}}{\lambda^{(j)}})}$$

where  $\lambda^{(j)}$  has been reintroduced. Other choices for the nonlinear weight function  $w$  are possible, however finding a good map that has both a closed-form log-determinant and inverse is non-trivial. Alternate weighting functions remain a direction for future research.

### 2.2.3. SET-NVP

Lastly, we propose a set-level scaling and shifting non-volume preserving (NVP) transformation (Dinh et al., 2016). For  $d$  dimensional points, the NVP transformation scales and shifts one subset,  $S \subset \{1, \dots, d\}$  of the  $d$  covariates given then rest,  $S^c$  as:

$$x^{(S)} \mapsto \exp \left( f \left( x^{(S^c)} \right) \right) x^{(S)} + g \left( x^{(S^c)} \right) \quad (20)$$

$$x^{(S^c)} \mapsto x^{(S^c)}, \quad (21)$$

for learned functions  $f$ , and  $g$ .

We propose to extend this mapping to sets, as follows:

$$x_i^{(S)} \mapsto \exp \left( f \left( \varphi(\mathbf{x}^{(S^c)}), x_i^{(S^c)} \right) \right) x_i^{(S)} \quad (22)$$

$$\begin{aligned} &+ g \left( \varphi(\mathbf{x}^{(S^c)}), x_i^{(S^c)} \right) \\ x_i^{(S^c)} &\mapsto x_i^{(S^c)}, \end{aligned} \quad (23)$$

where  $\varphi(\mathbf{x}^{(S^c)})$  is a permutation invariant Deepset representation. The embedding  $\varphi$  is responsible for capturing the

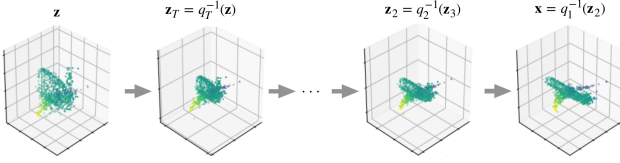


Figure 3. Transformation of a sample from the latent ( $\mathbf{z}$ ) to original ( $\mathbf{x}$ ) space. The composition of multiple transformations allows for a gradual flow of intraset dependencies from  $\mathbf{z}$  to  $\mathbf{x}$ .

set-level information from other covariates, which is then combined with each point  $x_i^{(S^c)}$  for shifts and scales that are both point and set level dependent. In this work, we take  $|S| = 1$ , transforming one dimension based on the rest, and composing in a round robin fashion. The log-determinant is given by  $f(\varphi(\mathbf{x}^{(S^c)}), x_i^{(S^c)})$  and the inverse by

$$z_i^{(S)} \mapsto \exp\left(-f\left(\varphi(\mathbf{z}^{(S^c)}), z_i^{(S^c)}\right)\right) \quad (24)$$

$$\times \left(z_i^{(S)} - g\left(\varphi(\mathbf{z}^{(S^c)}), z_i^{(S^c)}\right)\right) \\ z_i^{(S^c)} \mapsto z_i^{(S^c)}. \quad (25)$$

#### 2.2.4. POINTWISE TRANSFORMATIONS

In addition to the setwise transformations just introduced, we incorporate several pointwise transformations (12) to further capture point-level dependencies. Specifically, we use the linear map (Lin), leaky ReLU (L-ReLU), RNN coupling (RNN-C), shift, and reverse (Rev), typically applied before any set-wise permutation equivariant transformations. Details on these pointwise transformations can be found in (Oliva et al., 2018).

#### 2.2.5. COMPOSING TRANSFORMATIONS

To combine the strengths of each transformation and allow for dependencies to propagate through points and dimensions, we chain transformations together as  $q = q_T \circ \dots \circ q_1$ . The likelihood under  $T$  composed transformations factors with a product of respective Jacobian determinants:

$$p(\mathbf{x}) = \prod_{t=1}^T \left| \det \frac{dq_t}{dq_{t-1}} \right| \prod_{i=1}^d p\left(q(\mathbf{x})^{(i)} \mid q(\mathbf{x})^{(<i)}\right). \quad (26)$$

When each  $q_t$  is permutation equivariant, it is easy to show that the composition,  $q$ , is also permutation equivariant, thus preserving the exchangeability of the data. Figure 3 illustrates the inversion of transformations from the latent space to the input space.

### 2.3. Likelihoods

Now we turn our attention to constructing the likelihood component of our model (9),  $\prod_{i=1}^d p(\mathbf{z}^{(i)} \mid \mathbf{z}^{(<i)})$ . Recall that we are modeling our sets in a transformed space,  $\mathbf{z} = q(\mathbf{x})$ , however the likelihood models proposed below may be directly applied to the original space (where  $q$  is the identity  $\mathbf{z} = \mathbf{x}$ ).

Our main objective is to model data in a fashion that is invariant to permutation, yet is still dependent on relationships among points in the same set. This is particularly challenging for the first term in our factorization above,  $p(\mathbf{z}^{(1)})$ , which is unconditioned on the corresponding set of previous dimensions.

First, we propose methods that are able to model intradependencies in the unconditioned case. After, we shall develop a methodology of including conditioning information from the set of previous dimensions. Lastly, we propose an overarching variational autoencoding scheme to use on top of these likelihoods.

#### 2.3.1. MIXTURE OF MIXTURE MODEL

When modeling the likelihood of the first dimension,  $\mathbf{z}^{(1)}$ , we cannot condition on the previous dimensions and thus must take special care in modeling  $p(\mathbf{z}^{(1)})$  to preserve exchangeability. As mentioned, the simplest way to retain exchangeability in an unconditioned setting is to model the data in an *i.i.d.* fashion,  $p(\mathbf{z}^{(1)}) = \prod_{i=1}^n p(z_i^{(1)})$ . However, this implicitly assumes that every set starts with the same distribution. Such a model would leave the transformation to bear the complete burden of capturing intradependencies. Instead, we allow for multiple types of draws in the likelihood component in a model motivated by de Finetti’s theorem. The theorem states that an exchangeable infinite sequence of Bernoulli random variables can be modeled via a mixture of *i.i.d.* distributions:  $p(X_1, X_2, \dots) = \int p_\theta(X_1, X_2, \dots) d\theta$  (see (Bernardo & Smith, 2009) for more general extensions). Following de Finetti, we consider a density which is a finite mixture of *i.i.d.* distributions:

$$p(\mathbf{z}^{(1)}) = \sum_{k=1}^K \pi_k \prod_{i=1}^n p(z_i^{(1)} \mid \theta_k). \quad (27)$$

One must still specify  $p(z_i^{(1)} \mid \theta_k)$ . Here, we again use a mixture model, leading to a *mixture of mixtures*, i.e.  $\theta_k$  details the parameters of a mixture model with  $M$  components and a base distribution with shift and scaling parameters:

$$p(z_i^{(1)} \mid \theta_k) = \sum_{m=1}^M \pi_m(\theta_k) f(z_i^{(1)} \mid \mu_m(\theta_k), \sigma_m(\theta_k)).$$

Under the *mixture-of-mixtures* model, the distinct types of intradependencies among points are each encapsulated by a

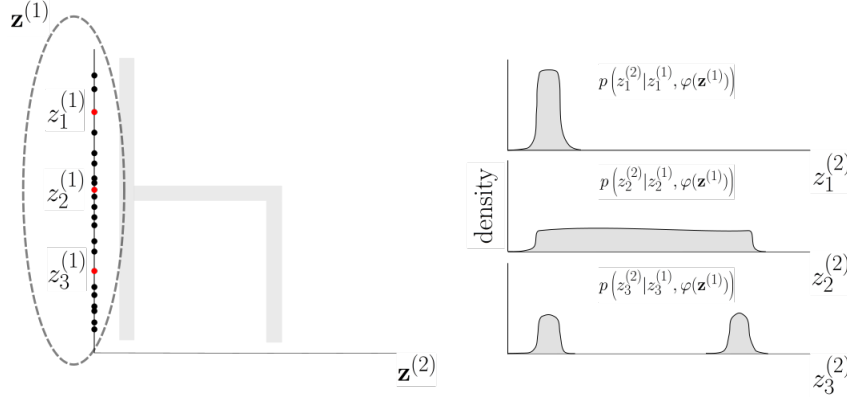


Figure 4. An illustration of how the PILET model’s conditional likelihoods capture set-level and point-level dependencies.  $\varphi(\mathbf{z}^{(1)})$  is a set-level embedding of  $\mathbf{z}^{(1)}$ , the circled set of points above.  $\varphi(\mathbf{z}^{(1)})$  tells the model aggregate properties of the distribution captured by the first dimension, specifying the global structure for the distribution of  $\mathbf{z}^{(2)}$ , while the point level information  $z_i^{(1)}$  specifies the distribution of  $z_i^{(2)}$  given  $\varphi(\mathbf{z}^{(1)})$ .

separate density  $p(\cdot|\theta_k)$ . The likelihood of generating a set  $\mathbf{z}^{(1)}$  is then the weighted likelihood (with priors  $\pi_k$ ) of generating the set according to each intradependency model  $p(\mathbf{z}^{(1)}|\theta_k)$ .

### 2.3.2. SET-CONDITIONED MODEL

In contrast to the unconditioned case  $p(\mathbf{z}^{(1)})$ , one has access to much more information when modeling set-likelihood given the previous dimensions  $p(\mathbf{z}^{(i)} | \mathbf{z}^{(<i)})$ . We make use of two additional levels of information: corresponding *point-level* information for the point  $z_j^{(i)}$  via  $z_j^{(<i)}$ , and aggregate *set-level* information via  $\mathbf{z}^{(<i)}$ .

As discussed, we require the likelihood to be permutation invariant in order to preserve exchangeability. We propose to achieve this by conditioning on a permutation invariant embedding of  $z_j^{(<i)}$ . For instance, we may take the conditional density to be:

$$p(\mathbf{z}^{(i)} | \mathbf{z}^{(<i)}) = \prod_{j=1}^n p\left(z_j^{(i)} | z_j^{(<i)}, \varphi(\mathbf{z}^{(<i)})\right), \quad (28)$$

where  $z_j^{(<i)}$  accounts for the point level dependence, and  $\varphi(\mathbf{z}^{(<j)})$  accounts for the set-level dependence. Here, (28) amounts to a model that is *i.i.d.* conditioned on the set-level information (see Figure 4).

### 2.3.3. COMPLETE LIKELIHOOD

Thus far we have discussed multiple ways of extending exchangeable models at the likelihood level over stringent *i.i.d.* assumptions. Inspired by de Finetti’s theorem, we propose the use of *mixture-of-mixtures*, which is able to generate sets from a bank of multiple distinct distributions. We also proposed to take advantage of additional point- and

set-level information by conditioning on permutation invariant set-embeddings. We combine these proposed methods throughout the conditional portion of our model (9):  $\prod_{i=1}^d p(\mathbf{z}^{(i)} | \mathbf{z}^{(<i)})$ . That is, we consider a set conditioned *mixture-of-mixtures* model for the conditional distribution of the  $i$ th dimension:

$$p(\mathbf{z}^{(i)} | \mathbf{z}^{(<i)}) = \sum_{k=1}^K \pi_k \left( \varphi(\mathbf{z}^{(<i)}) \right) \prod_{j=1}^n p_k \left( z_j^{(i)} | \varphi(\mathbf{z}^{(<i)}), z_j^{(<i)} \right), \quad (29)$$

where  $\varphi(\mathbf{z}^{(<i)})$  is a permutation invariant embedding.

## 2.4. PILET Model

As discussed, we make joint use of transformations of variables and conditional likelihoods to fully capture intradependences among the points and dimensions of a set (9). When composing various transformations, the output set of the previous transformation is used as the input for the next transformation (26). Then, the output of the last transformation  $\mathbf{z}$  is modeled using conditional densities (29) that make use of *mixture-of-mixtures* and set conditioning to yield likelihoods on the transformed space (29). The resulting log likelihood:

$$\log p(\mathbf{x}) = \sum_{t=1}^T \log \left| \det \frac{dq_t}{dq_{t-1}} \right| + \sum_{i=1}^d \log p \left( \mathbf{z}^{(i)} | \mathbf{z}^{(<i)} \right), \quad (30)$$

is optimized using a batch of multiple sets  $\mathbf{x}$ .

## 2.5. PILET-VAE Model

Finally, we propose to extend our model to make use of a latent code in an exchangeable variational autoencoder

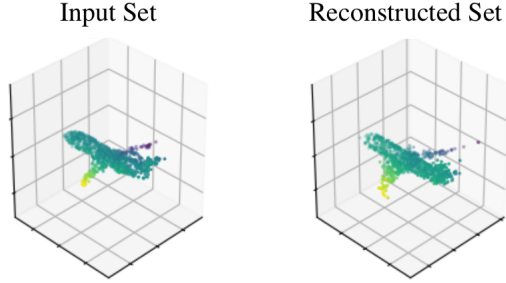


Figure 5. Reconstruction of a sample from its decoded VAE code using the PILET-VAE model.

(VAE) framework. Here set-likelihoods are conditioned on a latent variable:

$$p(\mathbf{x}) = \int p(\mathbf{x}|c)\pi(c)dc \quad (31)$$

where  $c$  is a latent “code”, with prior  $\pi(c)$ . We optimize the model using the standard variational lower-bound:

$$\log p(\mathbf{x}) \geq \mathbb{E}_{c \sim Q(\cdot|\mathbf{x})} [p(\mathbf{x}|c)] - \text{KL} [Q(\cdot|\mathbf{x}) || \pi(\cdot)], \quad (32)$$

where we take the proposal distribution to be a Gaussian conditioned on a permutation invariant embedding  $\phi(\mathbf{x})$ ,  $Q(\cdot|\mathbf{x}) = \mathcal{N}(\cdot|\bar{\mu}(\phi(\mathbf{x})), \text{diag} \bar{\sigma}^2(\phi(\mathbf{x})))$ , the prior  $\pi$  to be the standard Gaussian, and  $p(\mathbf{x}|c)$  to be our PILET model (9) conditioned on the additional code  $c$ . The extra conditioning on  $c$  propagates through the rest of our model by simply concatenating it to the (possibly empty) vector of conditioning values for each likelihood.

$p(\cdot|c)$  acts as a “decoder” for the set  $\mathbf{x}$ , which models the decoded set with intradependencies through the PILET model. The “encoder”  $Q(c|\mathbf{x})$  stems from a deepset embedding. Together, the encoder and decoder construct a powerful and effective autoencoder as can be seen below in Figure 5.

### 3. Experiments

We perform several experiments on synthetic and real data to illustrate the strengths of the PILET as well as the added modeling power offered by each component of the model. In the following sections, we demonstrate that the PILET model can learn: the ground truth likelihood of a distribution (3.1), how to sample effectively from complicated, real-world data distributions (3.2), and real-world distributions in a multi-class setting (3.3).

**Methods** In addition to PILET and PILET-VAE, we test two other versions of the model. This includes PILET without any transformations (NoTrans) and the BRUNO model (Korshunova et al., 2018). The BRUNO model can

be shown to be a basic case of the PILET model, expressed as a sequence of pointwise transformations followed by an L-PEq transformation with an unconditioned base distribution. We use  $6 \times \text{NVP}$ , Shift, and an L-PEq transformations with a Gaussian base in our implementation of BRUNO. For PILET and PILET-VAE, we apply the sequence of pointwise transformations Lin, L-ReLU, RNN-C, L-ReLU, Rev, RNN-C, L-ReLU, Lin, followed by the setwise transformations,  $2 \times (\text{Set-NVP}, \text{NW-PEq}, \text{Pointwise}(\text{Lin}, \text{L-ReLU}))$ , with Gaussian base distributions for the *mixture-of-mixtures* likelihoods. Experiments were implemented in Tensorflow<sup>2</sup> (Abadi et al., 2016).

#### 3.1. Synthetic Data

In our first experiment, we model the distribution of sets generated simulated from one of eight Gaussians with equal chance (a mixture of *i.i.d.* Gaussians). Details can be found in Appendix A. Learning from a known distribution allows us to compare the likelihood of the PILET model to that of the true underlying distribution. Each of the models tested learns to predict the log-likelihood of the synthetic dataset to within 1% of the known, ground truth likelihoods.

#### 3.2. ModelNet40: Airplanes and Chairs

Next we train the various PILET models on selected classes from a point-cloud version of the ModelNet40 dataset (Wu et al., 2015). The point clouds were created by randomly sampling 10,000 points from the surface of each object. In these experiments, models are trained separately on two subsets of the data: “airplanes” and “chairs,” using random sampling of 1,000 of the 10,000 points. Figure 6 illustrates random draws from BRUNO (6(a)) and PILET-VAE (6(b)) as trained on the airplanes class from ModelNet40.

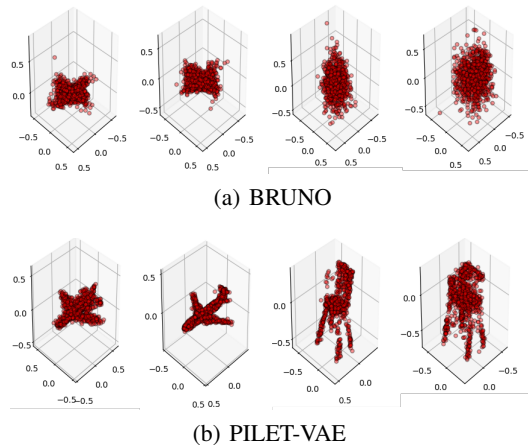


Figure 6. Samples from models trained on ModelNet40 airplanes (left two plots) and chairs (right two plots).

<sup>2</sup>Code can be found at <https://github.com/lupalab/pilet>.

### 3.3. Full ModelNet40 Dataset

Finally, we train each model on a training set that includes all 40 classes from the ModelNet40 dataset. We break the full dataset into two training cases. In one case, we train the data as if each of the classes came from the same underlying distribution. In the second case, we supply the class information in the form of a one-hot vector and require that the models estimate the conditional likelihood. A similar procedure is used during sampling for both cases. Figure 7 contains a random draw from three random ModelNet40 classes using the PILET model. Each of these examples is recognizable as belonging to the class that it was conditioned.

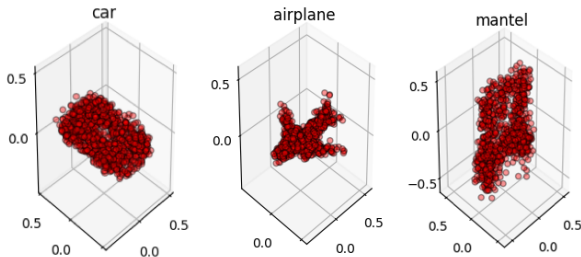


Figure 7. Label-conditioned samples from the PILET model.

### 4. Related Work

Several other works address likelihood estimation through transformation (Dinh et al., 2014; 2016; Kingma & Dhariwal, 2018), autoregression (Larochelle & Murray, 2011; Uria et al., 2013; 2016; Gregor et al., 2014; Germain et al., 2015), or a combination of both (Oliva et al., 2018); but none of these models address exchangeable data. Our work incorporates the transformation methods by separating data across dimension (instead of checkerboarding (Dinh et al., 2016)) to preserve permutation equivariance. We exploit conditioning by utilizing permutation equivariant operations at the set level.

Bayesian sets (Ghahramani & Heller, 2006) models exchangeable sets of binary features (Heller & Ghahramani, 2006). Unfortunately, the model does not allow for inverse operations which precludes the possibility of drawing new samples from the learned distributions. Our model does not require a binary map and is invertible so that novel samples can be drawn. Similar to the PILET model, the neural statistician (Edwards & Storkey, 2017) estimates a permutation invariant code produced by an exchangeable VAE. Sampling is performed by assuming that the data can be drawn independently given the VAE code  $x_i^{(j)} \sim p(x_i^{(j)}|c)$ . Our work extends this concept by allowing a VAE to condition a distribution that already models intraset dependencies. In fact, we may see from Figure 7 that PILET likelihoods are very expressive even without a VAE framework.

Table 1. Mean test log-likelihoods for ModelNet40 dataset.

Model	Airplane	Chair	All	All   Labels
PILET-VAE	<b>4.08</b>	<b>2.03</b>	<b>2.13</b>	<b>2.29</b>
PILET	3.75	1.47	1.58	1.94
NoTrans	3.49	1.04	1.37	1.82
BRUNO	2.60	0.79	0.75	0.64

As introduced earlier, the BRUNO model (Korshunova et al., 2018) explores a model which can be expressed as a stripped-down version PILET model. Omitting conditioning between dimensions and considering only pointwise transformations with a simple linear permutation equivariant transformation makes it difficult to accurately model complicated intradependencies of elements within input sets. This is evidenced by the superior performance of the PILET model shown in Table 1.

### 5. Discussion

We have introduced the PILET model for predicting likelihoods and sampling from exchangeable data.

Table 1 lists the log-likelihoods for the real datasets from each of the models. The likelihood values are all scaled by the number of points in each set (e.g. divided by 1,000). Scaling is performed since the input can have a differing number of points per set. The largest (best) value is emphasized in bold. Across each, PILET-VAE performs the best, attaining the highest mean log-likelihood. The success of PILET-VAE is made even clearer by the improvement in quality of samples over simpler models like NoTrans and BRUNO (see Appendix B). Figure 7 demonstrates that even without the added VAE, the PILET model produces high quality samples when conditioning on labeled data.

In this work, we have focused on applications to point clouds with the same number of points but the PILET model may be easily applied to sets in higher dimensions and with varying cardinality. Additional future work may consider more complex transformations with more sophisticated techniques for incorporating set- and point-level dependencies in the data.

In conclusion, our proposed framework, PILET, represents a substantial and novel push forward in machine learning methodology for unordered, exchangeable data. We developed several setwise transformations of variables (the non-linear weighted equivariant and set-NVP) and likelihood methods (the mixture-of-mixture, and set-conditional model) that are able to capture distinct intradependencies in points while naturally maintaining exchangeability. In addition, we also propose a VAE extension to these methods. Finally, we show the efficacy of our methods and their comprising components with experiments on both synthetic and real-world data.



## Acknowledgements

Kevin O’Connor would like to acknowledge the support of NIH grant T32 LM12420.

## References

- Abadi, M., Barham, P., Chen, J., Chen, Z., Davis, A., Dean, J., Devin, M., Ghemawat, S., Irving, G., Isard, M., et al. Tensorflow: a system for large-scale machine learning. In *OSDI*, volume 16, pp. 265–283, 2016.
- Bernardo, J. M. and Smith, A. F. *Bayesian theory*, volume 405. John Wiley & Sons, 2009.
- Dinh, L., Krueger, D., and Bengio, Y. Nice: Non-linear independent components estimation. *CoRR*, abs/1410.8516, 2014.
- Dinh, L., Sohl-Dickstein, J., and Bengio, S. Density estimation using real NVP. *CoRR*, abs/1605.08803, 2016.
- Edwards, H. and Storkey, A. Towards a neural statistician. In *5th International Conference on Learning Representations (ICLR 2017)*, 2 2017.
- Germain, M., Gregor, K., Murray, I., and Larochelle, H. MADE: Masked Autoencoder for Distribution Estimation. In Bach, F. and Blei, D. (eds.), *Proceedings of the 32nd International Conference on Machine Learning*, volume 37 of *Proceedings of Machine Learning Research*, pp. 881–889, Lille, France, 07–09 Jul 2015. PMLR.
- Ghahramani, Z. and Heller, K. A. Bayesian sets. In Weiss, Y., Schölkopf, B., and Platt, J. C. (eds.), *Advances in Neural Information Processing Systems 18*, pp. 435–442. MIT Press, 2006.
- Gregor, K., Danihelka, I., Mnih, A., Blundell, C., and Wierstra, D. Deep autoregressive networks. In Xing, E. P. and Jebara, T. (eds.), *Proceedings of the 31st International Conference on Machine Learning*, volume 32 of *Proceedings of Machine Learning Research*, pp. 1242–1250, Beijing, China, 22–24 Jun 2014. PMLR.
- Heller, K. A. and Ghahramani, Z. A simple bayesian framework for content-based image retrieval. In *Computer Vision and Pattern Recognition, 2006 IEEE Computer Society Conference on*, volume 2, pp. 2110–2117. IEEE, 2006.
- Kingma, D. P. and Dhariwal, P. Glow: Generative flow with invertible 1x1 convolutions. In *Advances in Neural Information Processing Systems*, pp. 10236–10245, 2018.
- Korshunova, I., Degraeve, J., Huszar, F., Gal, Y., Gretton, A., and Dambre, J. Bruno: A deep recurrent model for exchangeable data. In *Advances in Neural Information Processing Systems*, pp. 7190–7198, 2018.
- Larochelle, H. and Murray, I. The neural autoregressive distribution estimator. In Gordon, G., Dunson, D., and Dudk, M. (eds.), *Proceedings of the Fourteenth International Conference on Artificial Intelligence and Statistics*, volume 15 of *Proceedings of Machine Learning Research*, pp. 29–37, Fort Lauderdale, FL, USA, 11–13 Apr 2011. PMLR.
- Oliva, J. B., Dubey, A., Póczos, B., Schneider, J., and Xing, E. P. Transformation autoregressive networks. *arXiv preprint arXiv:1801.09819*, 2018.
- Qi, C. R., Su, H., Mo, K., and Guibas, L. J. Pointnet: Deep learning on point sets for 3d classification and segmentation. *Proc. Computer Vision and Pattern Recognition (CVPR), IEEE*, 1(2):4, 2017.
- Rezatofighi, S. H., Milan, A., Abbasnejad, E., Dick, A., Reid, I., et al. Deepsetnet: Predicting sets with deep neural networks. In *Computer Vision (ICCV), 2017 IEEE International Conference on*, pp. 5257–5266. IEEE, 2017.
- Uria, B., Murray, I., and Larochelle, H. Rnade: The real-valued neural autoregressive density-estimator. In Burges, C. J. C., Bottou, L., Welling, M., Ghahramani, Z., and Weinberger, K. Q. (eds.), *Advances in Neural Information Processing Systems 26*, pp. 2175–2183. Curran Associates, Inc., 2013.
- Uria, B., Côté, M.-A., Gregor, K., Murray, I., and Larochelle, H. Neural autoregressive distribution estimation. *Journal of Machine Learning Research*, 17(205): 1–37, 2016.
- Vinyals, O., Bengio, S., and Kudlur, M. Order matters: Sequence to sequence for sets. *arXiv preprint arXiv:1511.06391*, 2015.
- Wu, Z., Song, S., Khosla, A., Yu, F., Zhang, L., Tang, X., and Xiao, J. 3d shapenets: A deep representation for volumetric shapes. In *Proceedings of the IEEE conference on computer vision and pattern recognition*, pp. 1912–1920, 2015.
- You, J., Ying, R., Ren, X., Hamilton, W., and Leskovec, J. Graphrnn: Generating realistic graphs with deep autoregressive models. In *International Conference on Machine Learning*, pp. 5694–5703, 2018.
- Zaheer, M., Kottur, S., Ravanbakhsh, S., Poczos, B., Salakhutdinov, R. R., and Smola, A. J. Deep sets. In *Advances in Neural Information Processing Systems*, pp. 3391–3401, 2017.

## A. Synthetic Data Experiment Details

### A.1. Data Generation

For each generated set  $\mathbf{x}_i$ , we generate  $n = 1,000$  points  $x_{i1}, \dots, x_{in} \sim \mathcal{N}_3(\mu_i, \Sigma)$  where  $\Sigma = \sigma \mathbf{I}_3$  and  $\mu_i$  is a random draw of the eight vertices from an origin-centered cube with a side length of two. This is repeated  $N = 10,000$  times to obtain a dataset of 10,000 sets with 1,000 points and 3 dimensions. We experiment with  $\sigma = 1$  to allow some overlap between the components of the distribution.

### A.2. Ground Truth Likelihood

Since each of the eight sets is taken from an independent, 3d Gaussian, the mean log-likelihood of the dataset is straightforward to compute:

$$-\log(8) + \frac{1}{N} \sum_{i=1}^N \log \sum_{k=1}^8 \exp \left( \sum_{j=1}^n \sum_{d=1}^3 \left( x_{i,j}^{(d)} - \mu_k^{(d)} \right)^2 \right) - \frac{1}{2} \log \left( 2\pi\sigma_k^{(d)2} \right) - \frac{\left( x_{i,j}^{(d)} - \mu_k^{(d)} \right)^2}{2\sigma_k^{(d)2}} \quad (33)$$

We compare this to the mean log-likelihood of the test dataset obtained by the PILET model.

### A.3. Results

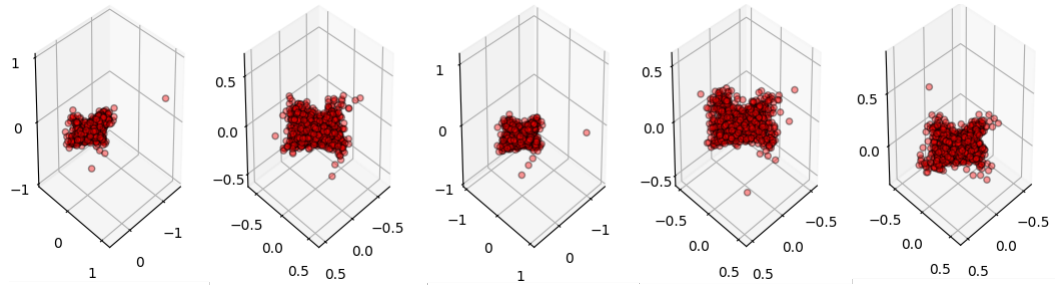
We report the mean test log-likelihoods from the synthetic data experiment in Table 2. Note that each model estimates the log-likelihood almost exactly.

Table 2. Mean test log-likelihoods for synthetic data.

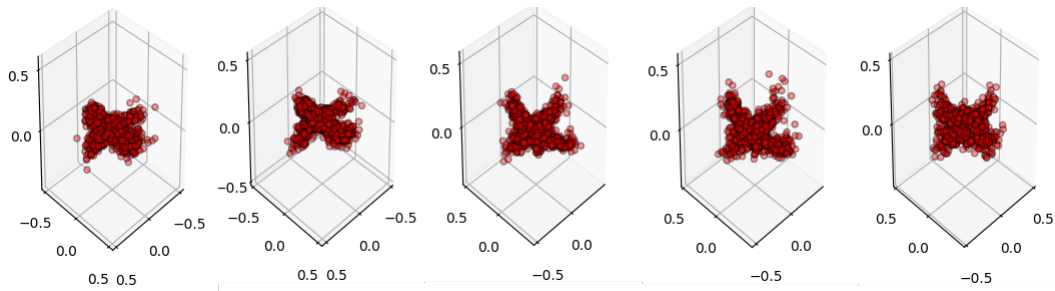
Model	Synthetic
PILET-VAE	-4.26
PILET	-4.26
NoTrans	-4.26
BRUNO	-4.27
<b>Ground Truth</b>	-4.26

## B. Example Airplane Samples

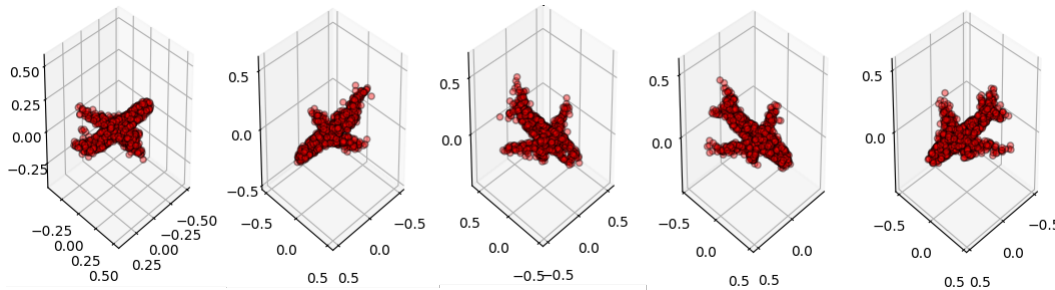
Figure 8 illustrates five random draws from each of our models trained on the ModelNet40 Airplane class.



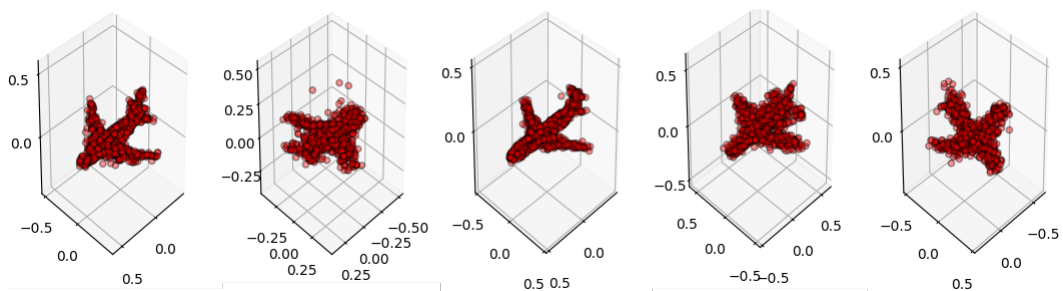
(a) Airplanes drawn from BRUNO



(b) Airplanes drawn from NoTrans



(c) Airplanes drawn from PILET



(d) Airplanes drawn from PILET-VAE

Figure 8. Samples from each model trained on the ModelNet40 Airplane class